Physics Letters B 749 (2015) 88–93

Contents lists available at ScienceDirect

Physics Letters B

www.elsevier.com/locate/physletb

Nuclear geometry effect and transport coefficient in semi-inclusive lepton-production of hadrons off nuclei

Na Liu [a,b,*], Wen-Dan Miao [a], Li-Hua Song [a,c], Chun-Gui Duan [a]

[a] Department of Physics, Hebei Normal University, Shijiazhuang 050024, PR China
[b] College of Mathematics and Physics, Shijiazhuang University of Economics, Shijiazhuang 050031, PR China
[c] College of Science, Hebei United University, Tangshan 063009, PR China

ARTICLE INFO

Article history:
Received 24 October 2014
Received in revised form 3 June 2015
Accepted 22 July 2015
Available online 26 July 2015
Editor: J.-P. Blaizot

Keywords:
Deep inelastic scattering
Quark energy loss
Hadron production

ABSTRACT

Hadron production in semi-inclusive deep-inelastic scattering of leptons from nuclei is an ideal tool to determine and constrain the transport coefficient in cold nuclear matter. The leading-order computations for hadron multiplicity ratios are performed by means of the SW quenching weights and the analytic parameterizations of quenching weights based on BDMPS formalism. The theoretical results are compared to the HERMES positively charged pions production data with the quarks hadronization occurring outside the nucleus. With considering the nuclear geometry effect on hadron production, our predictions are in good agreement with the experimental measurements. The extracted transport parameter from the global fit is shown to be $\hat{q} = 0.74 \pm 0.03$ GeV^2/fm for the SW quenching weight without the finite energy corrections. As for the analytic parameterization of BDMPS quenching weight without the quark energy E dependence, the computed transport coefficient is $\hat{q} = 0.20 \pm 0.02$ GeV^2/fm. It is found that the nuclear geometry effect has a significant impact on the transport coefficient in cold nuclear matter. It is necessary to consider the detailed nuclear geometry in studying the semi-inclusive hadron production in deep inelastic scattering on nuclear targets.

1. Introduction

Hadron production in semi-inclusive deep inelastic scattering of leptons from nuclei is a good tool to understand the parton propagation and hadronization processes in cold nuclear matter. In the semi-inclusive deep inelastic scattering on nuclei, a virtual photon from the incident lepton is absorbed by a quark within a nucleus, the highly virtual colored quark propagates over some distance through the cold nuclear medium, evolves subsequently into an observed hadron. It is expected that the hadron multiplicities observed in the scattering is sensitive to whether the hadronization occurs within or outside the nucleus in a semi-classical picture. Therefore, the detailed understanding of the parton propagation and hadronization processes in cold nuclear matter would greatly benefit the study of the jet-quenching and parton energy loss phenomena observed in ultra-relativistic heavy-ion collisions [1].

Hadron production in deep-inelastic scattering was first performed at SLAC [2] followed by EMC [3], E665 [4]. The more precise experimental measurements were reported by the HERMES [5–8] and CLAS [9,26]. The experimental data are usually presented in terms of the multiplicity ratio R_M^h, which is defined as the ratio of the number of hadrons h produced per deep-inelastic scattering event on a nuclear target with mass number A to that for a deuterium target. However, the experimental results on R_M^h were only a function of one kinematic variable (so-called one-dimensional dependences) except that a two-dimensional dependence was reported for a combined sample of charged pions [8]. Recently, the hadron multiplicities in semi-inclusive deep-inelastic scattering were measured on neon, krypton, and xenon targets relative to deuterium at an electron (positron)-beam energy of 27.6 GeV at HERMES [10]. The multiplicity ratios were measured in a two-dimensional representation for positively and negatively charged pions and kaons, as well as protons and antiprotons. The two-dimensional representation consists in a fine binning in one variable and a coarser binning in another variable. The published two-dimensional data will further help us to study the space (time) development of hadronization in more detail.

* Corresponding author.
E-mail addresses: Liuna@sjzue.edu.cn (N. Liu), miaowd@mail.hebtu.edu.cn (W.-D. Miao), songlh@mail.heuu.edu.cn (L.-H. Song), duancg@mail.hebtu.edu.cn (C.-G. Duan).

http://dx.doi.org/10.1016/j.physletb.2015.07.048

In our preceding articles, we have calculated the nuclear modifications of hadron production in semi-inclusive deep inelastic scattering in a parton energy loss model. By means of the short hadron formation time, the relevant data with quark hadronization occurring outside the nucleus are picked out from HERMES experimental results [8] on the one-dimensional dependence of the multiplicity ratio R_M^h as a function of the energy fraction z of the virtual photon carried away by the hadron. Our theoretical results show that the nuclear effects on parton distribution functions can be neglected. It is found that the theoretical results considering the nuclear modification of fragmentation functions due to quark energy loss are in good agreement with the selected experimental data. The obtained energy loss per unit length is 0.38 ± 0.03 GeV/fm for an outgoing quark by the global fit [11]. Furthermore, the leading-order computations on hadron multiplicity ratios for the production of positively and negatively charged pions and kaons are compared with the selected two-dimensional data from the HERMES experiment [10] by means of the hadron formation time [8,27], which is estimated from the Lund model. For the case where the quark hadronization occurs inside the nucleus [12], it is shown that with increase of the energy fraction carried by the hadron, the nuclear suppression on hadron multiplicity ratio from nuclear absorption gets bigger. The nuclear absorption is the dominant mechanism causing a reduction of the hadron yield. The atomic mass dependence of hadron attenuation is confirmed theoretically and experimentally to be proportional to $A^{1/3}$. For the case where the quark hadronization occurs outside the nucleus [13], the atomic mass number dependence is theoretically and experimentally in good agreement with the $A^{2/3}$ power law. It should be noted that in these studies, the outgoing quark energy loss is employed in the form of the mean energy loss. The length traveled by the quark in the nuclear matter is taken as the average path length $L = (3/4)R_A$ where R_A is the nuclear radius.

In this paper, we employ the two-dimensional data from HERMES on the multiplicity ratios for positively charged pions production on neon nucleus with respect to deuterium target [10], seeing that the CLAS data [9,26] are suitable for studying the hadron production inside the nuclei. The experimental data with quark hadronization occurring outside the nucleus are selected by means of the hadron formation time in order to investigate the quark energy loss in cold nuclear matter. Because the mean energy loss cannot reflect the dominant parton energy loss mechanism, the present study will use the Salgado–Wiedemann (SW) quenching weights [14], and the analytic parameterizations of quenching weights [28] based on Baier, Dokshitzer, Mueller, Peigné and Schiff (BDMPS) formalism [22]. In addition, the nuclear geometry effect on the extracted transport coefficient is investigated. It is hoped to gain new knowledge about quark energy loss in a cold nuclear medium.

The remainder of the paper is organized as follows. In Section 2, the brief formalism for the hadron multiplicity in semi-inclusive deep inelastic scattering on the nucleus and nuclear modification of the fragmentation functions owing to quark energy loss are described. In Section 3, The results and discussion obtained are presented. Finally, a summary is presented.

2. The hadron multiplicity in semi-inclusive deep inelastic scattering on nuclei

Hadron production in semi-inclusive deep inelastic scattering can be computed within the QCD improved parton model. At leading order in perturbative QCD, the hadron multiplicity is given by

$$\frac{1}{N_A^{DIS}}\frac{dN_A^h}{dzd\nu} = \frac{1}{\sigma^{lA}}\int dx \sum_f e_f^2 q_f^A(x, Q^2)\frac{d\sigma^{lq}}{dxd\nu} D_{f|h}^A(z, Q^2), \quad (1)$$

$$\sigma^{lA} = \int dx \sum_f e_f^2 q_f^A(x, Q^2)\frac{d\sigma^{lq}}{dxd\nu}, \quad (2)$$

where N_A^h (N_A^{DIS}) is the yield of semi-inclusive (inclusive) deep-inelastic scattering leptons on nuclei A, ν is the virtual photon energy, e_f is the charge of the quark with flavor f, $q_f^A(x, Q^2)$ is the nuclear quark distribution function with Bjorken variable x and photon virtuality Q^2, $D_{f|h}^A(z, Q^2)$ is the nuclear modified fragmentation function of a quark of flavor f into a hadron h. The differential cross section for lepton-quark scattering at leading order, $d\sigma^{lq}/dxd\nu$, is given by

$$\frac{d\sigma^{lq}}{dxd\nu} = Mx\frac{4\pi\alpha_{em}^2}{Q^4}[1 + (1-y)^2], \quad (3)$$

where M and α_{em} are respectively the nucleon mass and the fine structure constant, y is the fraction of the incident lepton energy transferred to the target.

In semi-inclusive deep inelastic scattering, the initially produced energetic quark will have to go through multiple scattering and induced gluon bremsstrahlung as it propagates through the medium. The induced gluon bremsstrahlung effectively reduces the leading parton energy. The quark energy fragmenting into a hadron shifts from $E = \nu$ to $E' = \nu - \Delta E$, which results in a rescaling of the energy fraction of the produced hadron:

$$z = \frac{E_h}{\nu} \longrightarrow z' = \frac{E_h}{\nu - \Delta E}, \quad (4)$$

where E_h and ΔE are respectively the measured hadron energy and the quark energy loss in the nuclear medium. The fragmentation function in the nuclear medium [15],

$$D_{f|h}^A(z, Q^2) = \int_0^{(1-z)\nu} d(\Delta E) P(\Delta E, \omega_c, L)\frac{1}{1 - \Delta E/\nu} D_{f|h}(z', Q^2), \quad (5)$$

where $D_{f|h}$ is the standard (vacuum) fragmentation function of a quark of flavor f into a hadron h, the characteristic gluon frequency $\omega_c = (1/2)\hat{q}L^2$, $P(\Delta E, \omega_c, L)$ denotes the probability for a quark with energy E to lose an energy ΔE which originates from the quark radiating gluons. This probability distribution, the so-called quenching weight, depends on the path length L covered by the hard quark in the nuclear medium and the transport coefficient $\hat{q}$.

Based on the above formalism, the path length L is fixed, only the transport coefficient $\hat{q}$ remains to be determined.

3. Results and discussion

In order to explore the outgoing quark energy loss, we will pick out the experimental data with quark hadronization outside the nucleus from the two-dimensional data on the multiplicity ratio R_M^h for positively charged pions production on neon nucleus in three z slices as a function of ν, and in five ν slices as a function of z [10]. Unlike our previous researches with using the mean path length $L = (3/4)R_A$, we set $t > 2R_A$ with the hadron formation time $t = z^{0.35}(1-z)\nu/\kappa$ ($\kappa = 1$ GeV/fm) [8,11,27], which is defined as the time between the moment that the quark is struck by the virtual photon and the moment that the prehadron is formed. This assumption can make sure that the hadron is produced outside target nucleus rather than inside the nucleus. Using the criterion, the number of points in selected experimental data is 4 for $R_M^{\pi^+}(\nu)$ for positively charged pions produced on neon target in the z region of $0.2 < z < 0.4$. For the multiplicity ratio $R_M^{\pi^+}$

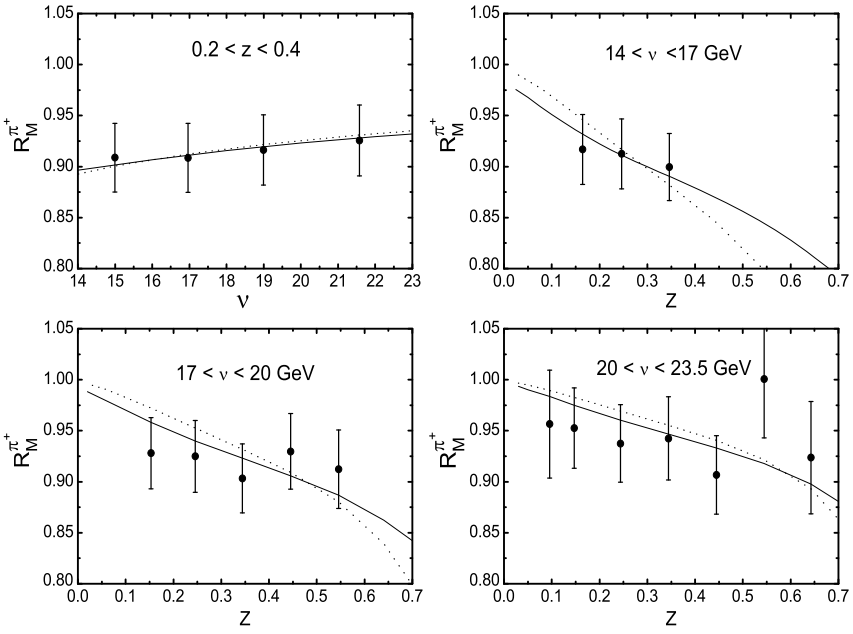

Fig. 1. The calculated multiplicity ratios $R_M^{\pi^+}$ in one ν slice and three z slices for positively charged pions production on neon target from the non-reweighted SW quenching weight (solid curves) and the parameterization of BDMPS quenching weight for the quark energy E independence (dotted curves). The HERMES data [10] are shown with the total uncertainty (statistical plus systematic, added quadratically).

Table 1
The values of $\hat{q}$ and χ^2/ndf extracted from the selected data on the hadron multiplicity ratios for positively charged pions produced on neon target by means of the SW quenching weights [14].

	Non-reweighted		Reweighted	
	$\hat{q}$ (GeV^2/fm)	χ^2/ndf	$\hat{q}$ (GeV^2/fm)	χ^2/ndf
	$L=(3/4)R_A$			
$0.2<z<0.4$	1.30 ± 0.06	0.02	1.44 ± 0.09	0.009
$14<\nu<17$	1.29 ± 0.05	0.13	1.44 ± 0.02	0.19
$17<\nu<20$	1.10 ± 0.09	0.53	1.14 ± 0.06	0.58
$20<\nu<23.5$	0.94 ± 0.06	0.62	0.94 ± 0.01	0.61
Global fit	1.15 ± 0.03	0.47	1.20 ± 0.02	0.54
	$L=\sqrt{R_A^2-b^2}-y$			
$0.2<z<0.4$	0.84 ± 0.02	0.013	1.02 ± 0.06	0.006
$14<\nu<17$	0.83 ± 0.04	0.05	1.07 ± 0.02	0.13
$17<\nu<20$	0.71 ± 0.05	0.37	0.79 ± 0.05	0.47
$20<\nu<23.5$	0.60 ± 0.05	0.53	0.60 ± 0.02	0.55
Global fit	0.74 ± 0.03	0.36	0.83 ± 0.02	0.46

as a function of z, there are 15 data points in three ν regions of $14<\nu<17$ GeV, $17<\nu<20$ GeV and $20<\nu<23.5$ GeV. In total, our analysis has 19 data points.

To comparing to the selected experimental data, we compute at leading order the hadron multiplicity ratios $R_M^{\pi^+}$,

$$R_M^{\pi^+}[\nu(z)] = \int \frac{1}{N_A^{DIS}} \frac{dN_A^h(\nu,z)}{dzd\nu} dz(\nu) \Big/ \int \frac{1}{N_D^{DIS}} \frac{dN_D^h(\nu,z)}{dzd\nu} dz(\nu). \tag{6}$$

In our calculation, the vacuum fragmentation functions [17] is employed together with the CTEQ6L parton density in the proton [16]. By means of the CERN subroutine MINUIT [18], the transport coefficient $\hat{q}$ is obtained by minimizing χ^2. One standard deviation of the optimum parameter corresponds to an increase of χ^2 by 1 unit from its minimum χ^2_{min}.

We use the SW quenching weight [14] in the soft multiple scattering approximation with the mean path length of the outgoing quark in the nuclear medium $L=(3/4)R_A$. In this case, the determined transport coefficient $\hat{q}$ and χ^2 per number of degrees of freedom (χ^2/ndf) are summarized in Table 1 for positively charged pions production on neon nuclei in a z slice and in three ν slices from the HERMES experiments [10]. The solid curves in Fig. 1 are our numeric results which are compared with the selected experimental data. It is shown that the computed hadron multiplicity ratio increases with ν, and decreases with z. It is found that the theoretical results are in good agreement with the experimental data. The global fit of all data makes $\hat{q}=1.15\pm0.03$ GeV^2/fm with the relative uncertainty $\delta\hat{q}/\hat{q}\simeq 2.6\%$ and $\chi^2/ndf=0.47$.

In above calculation, the employed quenching weight is computed in the eikonal limit of very large quark energy [14]. For the case of realistic initial quark energy, the finite energy correction need to be taken into account. To illustrate the theoretical uncertainty associated with finite energy corrections, we shall compare results without such corrections to those from the reweighted probability [19]

$$P_{rw}(\Delta E/\omega_c, L) = \frac{P(\Delta E/\omega_c, L)}{\int_0^{\nu/\omega_c} d(\Delta E/\omega_c) P(\Delta E/\omega_c, L)} \Theta(1-\Delta E/E). \tag{7}$$

Regarding the reweighted quenching weight, the global fit of all data gives $\hat{q}=1.20\pm0.02$ GeV^2/fm with the relative uncertainty $\delta\hat{q}/\hat{q}\simeq 1.6\%$ and $\chi^2/ndf=0.54$ (see Table 1). It is clear that the determined transport coefficient $\hat{q}$ is about 4% greater than that from non-reweighted quenching weight.

Now let us to study the nuclear geometry effect in the semi-inclusive lepto-production of hadrons off nuclei. The nuclear geometry is described by the nuclear density distribution $\rho_A(\vec{b},y)$, where y is the coordinate along the direction of the outgoing quark and $\vec{b}$ its impact parameter. The center of the target nucleus lies at $(\vec{0},0)$ (see Fig. 2). If we assume that the interaction of the virtual photon with the quark is located at $(\vec{b},y)$, the colored quark produced at y will travel the path length $L=\sqrt{R_A^2-b^2}-y$, along a direction with impact parameter $\vec{b}$. Then the averaged modified fragmentation function [20,27,29] should be

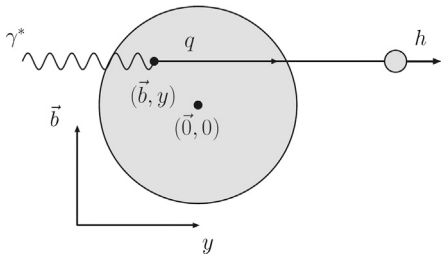

Fig. 2. Illustration of the geometry of hadron production in deeply inelastic scattering in the nucleus target rest frame. See details in text.

$$D^A_{f|h}(z, Q^2) = \int d^2b dy \rho_A(\vec{b}, y) \times \int_0^{(1-z)\nu} d(\Delta E) P(\Delta E, \omega_c, L) \frac{1}{1-\Delta E/\nu} \times D_{f|h}(z', Q^2). \quad (8)$$

For simplicity, we use the uniform hard-sphere nuclear density normalized to unity, $\rho_A(\sqrt{b^2+y^2}) = (\rho_0/A)\Theta(R_A - \sqrt{b^2+y^2})$ with ρ_0 is the nuclear density, $R_A = r_0 A^{1/3}$, and $r_0 = 1.12$ fm. By combining Eq. (8) and Eq. (1), the calculated corresponding transport coefficient $\hat{q}$ and χ^2 per number of degrees of freedom (χ^2/ndf) are summarized in Table 1 with the reweighted and non-reweighted quenching weights. It is shown that the global fit of all data gives separately $\hat{q} = 0.74 \pm 0.03$ GeV^2/fm with the relative uncertainty $\delta\hat{q}/\hat{q} \simeq 4.0\%$ and $\chi^2/ndf = 0.36$ for the non-reweighted quenching weight, and $\hat{q} = 0.83 \pm 0.02$ GeV^2/fm with the relative uncertainty $\delta\hat{q}/\hat{q} \simeq 2.4\%$ and $\chi^2/ndf = 0.46$ for the reweighted quenching weight. It is obvious that the nuclear geometry effect could reduce the transport coefficient by as much as 36% for the non-reweighted quenching weight and 31% for the reweighted quenching weight, respectively.

As can be seen from Table 1, the values of $\hat{q}$ are too high to be understandable in perturbation theory. The reason is that the coefficient of the discrete part $p_0\delta(\Delta E)$ of the quenching weight, p_0, is very large when using the finite-length medium in the SW quenching weights. The calculated value of p_0 reveals that p_0 ($\hat{q} = 0.8$ GeV^2/fm) reduces nonlinearly from 1.07 to 0.2 in the range $1.0 \le L \le 6.0$ fm ($2R_{Ne} \simeq 6.0$ fm). As for the same L, p_0 decreases as the increase of $\hat{q}$. Therefore, the small-L SW quenching weights result in the large values for $\hat{q}$.

The SW quenching weight evolves from the BDMPS calculation to include finite-length effects. The original BDMPS calculation takes a limit in which the nuclear medium length goes to infinity [22]. The analytic parameterization was given for BDMPS quenching weight [28]. The quenching weight $P(\Delta E)$ for the quark energy E independence follows with a great accuracy a log-normal distribution,

$$\bar{P}(\bar{\Delta E} = \Delta E/\omega_c) = \omega_c P(\Delta E) = \frac{1}{\sqrt{2\pi}\sigma\,\bar{\Delta E}} \exp\left[-\frac{\left(\log\bar{\Delta E} - \mu\right)^2}{2\sigma^2}\right], \quad (9)$$

with $\mu = -1.5$ and $\sigma = 0.73$. The quenching weight $P(\bar{\Delta E}, \bar{E})$ for the quark energy dependence follows

$$\bar{P}(\bar{\Delta E}, \bar{E}) = \frac{1}{\sqrt{2\pi}\,\sigma(\bar{E})\,\bar{\Delta E}} \exp\left[-\frac{\left(\log\bar{\Delta E} - \mu(\bar{E})\right)^2}{2\sigma(\bar{E})^2}\right] \quad (10)$$

where the $\mu(\bar{E})$ and $\sigma(\bar{E})$ are given by the empirical laws

Table 2
The values of $\hat{q}$ and χ^2/ndf extracted from the selected data on the hadron multiplicity ratios for positively charged pions produced on neon target by means of the analytic parameterizations of quenching weights [28].

	E independence		E dependence	
	$\hat{q}$ (GeV^2/fm)	χ^2/ndf	$\hat{q}$ (GeV^2/fm)	χ^2/ndf
	$L = (3/4)R_A$			
$0.2 < z < 0.4$	0.38 ± 0.07	0.04	0.41 ± 0.09	0.03
$14 < \nu < 17$	0.37 ± 0.07	0.51	0.40 ± 0.09	0.52
$17 < \nu < 20$	0.26 ± 0.05	0.98	0.27 ± 0.06	1.00
$20 < \nu < 23.5$	0.20 ± 0.06	0.79	0.21 ± 0.07	0.79
Global fit	0.29 ± 0.03	0.83	0.30 ± 0.04	0.84
	$L = \sqrt{R_A^2 - b^2} - y$			
$0.2 < z < 0.4$	0.26 ± 0.05	0.04	0.30 ± 0.06	0.02
$14 < \nu < 17$	0.25 ± 0.05	0.33	0.29 ± 0.07	0.38
$17 < \nu < 20$	0.19 ± 0.04	0.84	0.20 ± 0.05	0.88
$20 < \nu < 23.5$	0.15 ± 0.04	0.74	0.15 ± 0.04	0.76
Global fit	0.20 ± 0.02	0.70	0.22 ± 0.02	0.74

$$\mu(\bar{E}) = -1.5 + 0.81 \times \left(\exp\left(-0.2/\bar{E}\right) - 1\right),$$
$$\sigma(\bar{E}) = 0.72 + 0.33 \times \left(\exp\left(-0.2/\bar{E}\right) - 1\right). \quad (11)$$

The analytic parameterization $P(\bar{\Delta E}, \bar{E})$ reproduces qualitatively the characteristics of the E dependence of the mean energy loss $< \Delta E >$ from BDMPS formalism [30], e.g., the mean energy loss $< \Delta E > \propto \sqrt{\hat{q}EL}$ at small quark energy ($E < \omega_c$).

Taking advantage of the analytic parameterizations of quenching weights without and with the quark energy E dependence, the computed transport coefficient $\hat{q}$ and χ^2 per number of degrees of freedom (χ^2/ndf) are listed in Table 2. The expected multiplicity ratios $R_M^{\pi^+}$ (dotted curves) with $L = (3/4)R_A$ for the quenching weight of quark energy E independence, are in good agreement with the selected experimental data in Fig. 1. It is shown in Table 2 that the smaller values of $\hat{q}$ are given with comparing the SW quenching weights. The obtained value of $\hat{q}$ should be much more realistic from the BDMPS quenching weights.

As can be shown from Table 2, the global fit of all data by the quark energy E independent quenching weight gives separately $\hat{q} = 0.29 \pm 0.03$ GeV^2/fm with $\chi^2/ndf = 0.83$ from the mean length, and $\hat{q} = 0.20 \pm 0.02$ GeV^2/fm with $\chi^2/ndf = 0.70$ from the nuclear geometry effect. For the quark energy E independent and dependent quenching weight, the values of $\hat{q}$ from the global fit are consistent in 1σ range with (without) the nuclear geometry effect. Moreover, the nuclear geometry effect could reduce the transport coefficient by as much as 31% and 27% respectively. Therefore, we should consider the nuclear geometry effect over the course of studying the semi-inclusive hadron production in deep inelastic scattering on nuclear targets.

What we notice is in Table 2 that the extracted values of $\hat{q}$ are consistent within 1σ range by fitting the selected experimental data in the z region of $0.2 < z < 0.4$, and in two ν regions of $14 < \nu < 17$ GeV and $17 < \nu < 20$ GeV. However, in $20 < \nu < 23.5$ GeV region, the smaller value of $\hat{q}$ are given in comparison with those in other three kinematic ranges. The reason is that in $20 < \nu < 23.5$ GeV region, the value of $R_M^{\pi^+}(z = 0.54)$ deviates normal trend obviously (see Fig. 1). If we remove this experimental data point, the calculated values of $\hat{q}$ are respectively 0.18 ± 0.05 GeV^2/fm ($\chi^2/ndf = 0.42$, E independent quenching weight) and 0.19 ± 0.06 GeV^2/fm ($\chi^2/ndf = 0.43$, E dependent quenching weight) with considering the nuclear geometry effect. Then the obtained values of $\hat{q}$ can be consistent within 1σ range for the collected experimental data in four kinematic regions. Hence, the precise experimental data can refine our theoretical model.

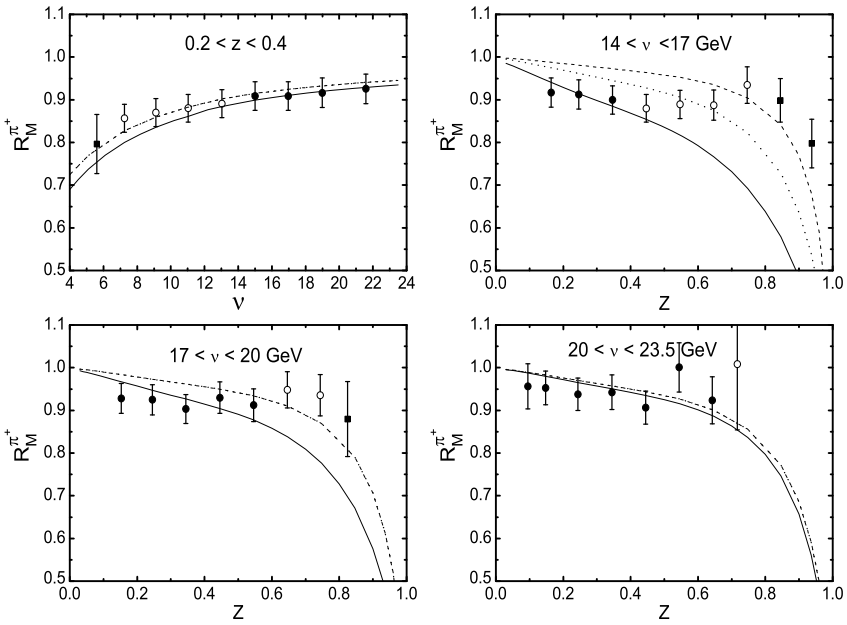

Fig. 3. The multiplicity ratios $R_M^{\pi^+}$. The solid, dotted and dashed lines correspond to the computed results by fitting the selected data ($t > 2R_A$, filled circles), the collected data ($2t > 2R_A$, filled and empty circles) and the full data, respectively.

Table 3
The values of $\hat{q}$ and χ^2/ndf extracted from the selected data ($2t > 2R_A$) and the full data on the hadron multiplicity ratios for positively charged pions produced on neon target by considering the nuclear geometry effect ($L = \sqrt{R_A^2 - b^2} - y$) and using the analytic parameterization of BDMPS quenching weight for the quark energy E independence [28].

	$2t > 2R_A$		Full data	
	$\hat{q}$ (GeV^2/fm)	χ^2/ndf	$\hat{q}$ (GeV^2/fm)	χ^2/ndf
$0.2 < z < 0.4$	0.22 ± 0.02	0.24	0.22 ± 0.02	0.24
$14 < \nu < 17$	0.12 ± 0.02	2.70	0.06 ± 0.01	3.98
$17 < \nu < 20$	0.10 ± 0.03	1.77	0.10 ± 0.02	1.59
$20 < \nu < 23.5$	0.13 ± 0.04	0.76	0.13 ± 0.04	0.76
Global fit	0.146 ± 0.01	1.40	0.109 ± 0.01	2.59

In this work, the hadron formation time, $t = z^{0.35}(1-z)\nu/\kappa$, is quoted from HERMES Collaboration [8]. This idea was pursued in Ref. [27]. The convenient parametrization can give its values as a function of z closely resembling the ones obtained in the Lund model [31]. However, the kinematic dependence for the formation time as well as its magnitude is not clearly known. To investigate the sensitivity of $\hat{q}$ values on the hadron formation time, our analysis is repeated by multiplying the formation time by 2 and 1/2 in order to select more or less data. It is found that there is no experimental data on $R_M^{\pi^+}$ that meet the criteria of $(1/2)t > 2R_A$ for positively charged pions produced on neon target in the z region of $0.2 < z < 0.4$, and in three ν regions of $14 < \nu < 17$ GeV, $17 < \nu < 20$ GeV and $20 < \nu < 23.5$ GeV. By using $2t > 2R_A$, 30 data points are selected in total for the corresponding four kinematic regions (see Fig. 3). By considering the nuclear geometry effect and using the analytic parameterization of BDMPS quenching weight without the quark energy E dependence, the computed transport coefficient $\hat{q}$ and χ^2/ndf are summarized in Table 3. For completeness, meanwhile, the values of $\hat{q}$ and χ^2/ndf are given in Table 3 by fitting the full experimental data (34 data points, see Fig. 3) in four kinematic regions. The calculated results are compared with the experimental data on multiplicity ratios in Fig. 3. The dotted and dashed lines are the results on multiplicity ratios by fitting the selected data ($2t > 2R_A$) and the full data, respectively. For convenient for comparing, the calculated multiplicity ratios are presented in Fig. 3 (solid lines) by using the selected data ($t > 2R_A$).

As can be seen from Table 3 and Fig. 3, the extracted values of $\hat{q}$ are identical except the region $14 < \nu < 17$ GeV for the selected data ($2t > 2R_A$) and the full data. In the range $14 < \nu < 17$ GeV, the theoretical values of χ^2/ndf are 2.70 ($2t > 2R_A$) and 3.98 (full data) separately. Moreover, the extracted value of $\hat{q}$ from the selected data ($2t > 2R_A$) is bigger than that from the full data. For the selected data ($t > 2R_A$), the collected data ($2t > 2R_A$) and the full data, as a whole, the values of $\hat{q}$ by the global fit are 0.20 ± 0.02 GeV^2/fm ($\chi^2/ndf = 0.70$), 0.146 ± 0.01 GeV^2/fm ($\chi^2/ndf = 1.40$) and 0.109 ± 0.01 GeV^2/fm ($\chi^2/ndf = 2.59$), respectively. As the included experimental data point increases, the extent of hadron absorption contamination become bigger. Additionally, the degree of the accordance with experimental data become worse. Although this assumption $t > 2R_A$ results in a too drastic data selection, the selection criteria can make sure that the hadron is produced outside target nucleus. Up to now, the formation time is yet an open question. In order to learn about the quark energy loss, on the one hand the in-depth study of the formation time is necessary in theory, but on the other the much higher energy experiments are expected to isolate the parton energy loss from any possible pre-hadron absorption effects.

It is worthy of note that our obtained transport coefficients are larger than Accardi's fit of $\hat{q} = 0.5$ GeV^2/fm [20,29] and Dupré's fit of $\hat{q} = 0.4$ GeV^2/fm [26] at the center of a target nucleus by using SW quenching weight. As for the quenching weights based on BDMPS formalism, our results are bigger than Arleo's value of $\hat{q} = 0.14$ GeV^2/fm [21]. In addition, Deng and Wang applied the modified DGLAP evolution to quark propagation in the deep inelastic scattering of a large nucleus within the framework of generalized factorization for higher-twist contributions to multiple parton scattering. The extracted jet transport parameter at the center of a large nucleus is found to be $\hat{q} = 0.024 \pm 0.008$ GeV^2/fm [23]. However, these research did not include χ^2 analysis, and did not distinguish whether the hadronization occurs within or outside the nucleus for the experimental data.

It is worth stressing that BDMPS evaluated the parton energy loss in the multiple-soft scattering approximation, and took a limit

in which the medium length goes to infinity. Salgado and Wiedemann improved the BDMPS calculation to include finite-length effects with the multiple gluon emission using a Poisson ansatz. The Higher-Twist formalism given by Wang and Guo [24,25] is another framework of the parton energy loss. However, the obtained transport parameter from the three set of parton energy loss calculations exists a significant difference in magnitude. The similar discrepancies between different parton energy loss formalisms are found in case of heavy-ion collisions [32,33]. Therefore, the theoretical progresses should be made furthermore. With future precision and much higher energy semi-inclusive deep-inelastic scattering experiment and theoretical advances in the parton energy loss, it should be possible to achieve a truly quantitative understanding of the parton energy loss mechanism.

4. Summary

We study the hadron production from semi-inclusive lepton-nucleus deep inelastic scattering, supplementing the perturbative QCD factorized formalism with radiative parton energy loss. The experimental data with the quark hadronization occurring outside the nucleus are selected against the following criterion: the hadron formation time is more than twice the nuclear radius. The fragmentation functions are modified with considering the energy loss incurred by hard quarks propagating through the nuclear medium by means of SW quenching weights and the analytic parameterizations of quenching weights based on BDMPS formalism. The leading order calculation of semi-inclusive hadron production on nuclei has been done, and compared with the selected HERMES experimental data. In a condition of considering the nuclear geometry effect on the semi-inclusive hadron production, a good agreement between our predictions and the experimental measurements is observed. The extracted transport parameter from the global fit is found to be $\hat{q} = 0.74 \pm 0.03$ GeV^2/fm for the SW quenching weight without the finite energy corrections. By using the analytic parameterization of BDMPS quenching weight without the quark energy E dependence, the computed transport coefficient is $\hat{q} = 0.20 \pm 0.02$ GeV^2/fm. It is found that the nuclear geometry effect has a significant impact on the transport coefficient in cold nuclear matter. Therefore, we should consider the nuclear geometry effect in studying the semi-inclusive hadron production in deep inelastic scattering on nuclear targets. In particular, we emphasized that the semi-inclusive hadron production on nuclei may help us to determine and constrain the transport coefficient (hence the quark energy loss) in cold nuclear matter. Furthermore, a better understanding of the parton energy loss mechanism can be achieved in the future.

Acknowledgements

We are greatly indebted to the anonymous referees for insightful suggestions that enabled us to develop a more comprehensive study. Na Liu is grateful to François Arleo for useful discussion. This work was supported in part by the National Natural Science Foundation of China (11075044, 11347107) and Natural Science Foundation of Hebei Province (A2008000137, A2013209299).

References

[1] A. Accardi, et al., Riv. Nuovo Cimento 32 (2010) 439.
[2] L. Osborne, et al., Phys. Rev. Lett. 40 (1978) 1624.
[3] J. Ashman, et al., EMC Collaboration, Z. Phys. C 52 (1991) 1.
[4] M. Adams, et al., E665 Collaboration, Phys. Rev. D 50 (1994) 1836.
[5] A. Airapetian, et al., HERMES Collaboration, Eur. Phys. J. C 20 (2001) 479.
[6] A. Airapetian, et al., HERMES Collaboration, Phys. Lett. B 577 (2003) 37.
[7] A. Airapetian, et al., HERMES Collaboration, Phys. Rev. Lett. 96 (2006) 162301.
[8] A. Airapetian, et al., HERMES Collaboration, Nucl. Phys. B 780 (2007) 1.
[9] A. Daniel, et al., CLAS Collaboration, Phys. Lett. B 706 (2011) 26.
[10] A. Airapetian, et al., HERMES Collaboration, Eur. Phys. J. A 47 (2011) 113.
[11] Li-Hua Song, Chun-Gui Duan, Phys. Rev. C 81 (2010) 035207.
[12] Li-Hua Song, Na Liu, Chun-Gui Duan, Chin. Phys. C 37 (2013) 104102.
[13] Li-Hua Song, Na Liu, Chun-Gui Duan, Chin. Phys. C 37 (2013) 084102.
[14] C.A. Salgado, U.A. Wiedemann, Phys. Rev. D 68 (2003) 014008.
[15] X.N. Wang, Z. Huang, I. Sarcevic, Phys. Rev. Lett. 77 (1996) 231.
[16] J. Pumplin, et al., J. High Energy Phys. 07 (2002) 012.
[17] M. Hirai, S. Kumano, T.-H. Nagai, K. Sudoh, Phys. Rev. D 75 (2007) 094009.
[18] F. James, CERN Program Library Long Writeup D506.
[19] C.A. Salgado, U.A. Wiedemann, Phys. Rev. Lett. 93 (2004) 042301.
[20] A. Accardi, talk at "From RHIC to LHC: achievements and opportunities", INT, Seattle, 17 October 2006.
[21] F. Arleo, Eur. Phys. J. C 30 (2003) 213.
[22] R. Baier, Y.L. Dokshitzer, A.H. Mueller, S. Peigne, D. Schiff, Nucl. Phys. B 484 (1997) 265.
[23] Wei-Tian Deng, Xin-Nian Wang, Phys. Rev. C 81 (2010) 024902.
[24] X.-N. Wang, X.-f. Guo, Nucl. Phys. A 696 (2001) 788.
[25] A. Majumder, arXiv:0901.4516 [nucl-th].
[26] Raphaël Dupré, Ph.D. thesis, Jefferson Lab, 2011, http://inspirehep.net/record/1206790/files/TH2011_Dupre_Raphael.pdf.
[27] A. Accardi, Eur. Phys. J. C 49 (2007) 347.
[28] F. Arleo, J. High Energy Phys. 0211 (2002) 044, arXiv:hep-ph/0210104v3.
[29] A. Accardi, Acta Phys. Hung. A 27 (2006) 189, arXiv:nucl-th/0510090.
[30] R. Baier, Y.L. Dokshitzer, A.H. Mueller, S. Peigné, D. Schiff, Nucl. Phys. B 483 (1997) 291, arXiv:hep-ph/9607355.
[31] A. Bialas, M. Gyulassy, Nucl. Phys. B 291 (1987) 793.
[32] N. Armesto, et al., Phys. Rev. C 86 (2012) 064904, arXiv:1106.1106 [hep-ph].
[33] Karen M. Burke, et al., Phys. Rev. C 90 (2014) 014909, arXiv:1312.5003 [nucl-th].